

Effects of nucleon-nucleon short-range correlations on inclusive electron scatteringQinglin Niu,¹ Jian Liu^{①,1,2,3,*} Yuanlong Guo,¹ Chang Xu,⁴ Mengjiao Lyu,⁵ and Zhongzhou Ren⁶¹College of Science, China University of Petroleum (East China), Qingdao 266580, China²Laboratory of High Precision Nuclear Spectroscopy, Institute of Modern Physics, Chinese Academy of Sciences, Lanzhou 730000, China³Guangxi Key Laboratory of Nuclear Physics and Nuclear Technology, Guangxi Normal University, Guilin 541004, China⁴Department of Physics, Nanjing University, Nanjing 210093, China⁵College of Science, Nanjing University of Aeronautics and Astronautics, Nanjing 210016, China⁶School of Physics Science and Engineering, Tongji University, Shanghai 200092, China

(Received 7 March 2022; accepted 15 April 2022; published 23 May 2022)

The nucleon-nucleon short-range correlation (NN -SRC) is one of the key issues of nuclear physics, which typically manifest themselves in high-momentum components of the nuclear momentum distributions. In this paper, the nuclear spectral functions based on the axially deformed relativistic mean-field model are developed to involve the NN -SRC. With the spectral functions, the inclusive electron scattering (e, e') cross sections are calculated within the plane-wave impulse approximation (PWIA) framework, including the quasielastic (QE) part and Δ production part. Especially in the Δ production region, we reconsider the electromagnetic structures of the nucleon resonance $\Delta(1232)$ and the scattering mechanisms, and thereby the theoretical calculations are improved effectively and the cross sections are well consistent with the experimental data. The theoretical (e, e') cross sections are further divided into NN -SRC and mean-field contributions. It is found that, at the kinematics $0.5 \text{ GeV}^2 < Q^2 < 1 \text{ GeV}^2$, the QE peak and Δ production peak not only reflect the mean-field structure but also are sensitive to the NN -SRC information. Finally, we provide another method to extract the strengths of NN -SRC from experimental cross sections for selected nuclei at the suitable kinematics.

DOI: [10.1103/PhysRevC.105.L051602](https://doi.org/10.1103/PhysRevC.105.L051602)

Introduction. Many-body Fermi systems including the short-range correlation (SRC) are common in nature, such as nuclear matter system and finite nuclei. The information on nucleon-nucleon short-range correlation (NN -SRC) is useful to answer several key issues about the properties of matter at high densities, such as neutron stars and relativistic heavy-ion collisions [1,2]. The research of the European Muon Collaboration (EMC) effect would benefit from the details of NN -SRC, which describes the modification of the quark-gluon structure of a nucleon bound in an atomic nucleus by the surrounding nucleons [3].

The information on NN -SRC can be obtained by new experimental data on electron scattering off nuclei. Corresponding experiments have been carried out at the Jefferson Laboratory [4–6], which are categorized into two groups: the exclusive electron scattering ($e, e'p$) and the inclusive electron scattering (e, e'). Previous measurements of ($e, e'p$) experiments on ^{12}C to ^{208}Pb [7,8] pointed out that there are approximately 20 times as many np -SRC pairs as there are pp -SRC and nn -SRC pairs, which originate from the tensor part of the nuclear force [9]. The (e, e') experiments have shown that SRC pair nucleons are shifted from low-momentum states to high-momentum states [10]. According to the (e, e') experiments at SLAC and Jefferson Laboratory [11–13], the ratios of (e, e') cross sections on heavy nuclei to those of the deuteron exhibit a plateau, at the squared four-momentum

transfer $Q^2 > 1.4 \text{ GeV}^2$ and large Bjorken scaling variable $1.5 < x_B < 2$. The plateau indicates that the high-momentum components of different nuclei have a similar shape, and the value of the plateau provides a chance to extract the proportion of high-momentum nucleons. As the development of experiment mentioned above, new theoretical works in the field of electron scattering are also stimulated to explain the experimental phenomenon and extract the information of nuclear structure information.

The plane-wave impulse approximation (PWIA) is a convenient theory widely applied to explain the quasielastic (QE) scattering and Δ production scattering [14]. Within the PWIA framework, the spectral function can be introduced into the descriptions of the (e, e') scattering reaction. The spectral function $S(\mathbf{p}, E)$ is the probability of finding a nucleon with given momentum \mathbf{p} and removal energy E in nuclei [14]. The (e, e') cross sections can be obtained by the two physical quantities: the spectral functions $S(\mathbf{p}, E)$ representing the nuclear structure, and the elementary cross section σ_{eN} describing the process of an electron scattered by an off-shell nucleon. It is a key problem for (e, e') scattering to calculate the elementary cross section, which depends on the information the electromagnetic structure of the nucleon. For the QE region, the cross sections have been well reproduced at the quantitative level. However, because of the uncertainties associated with the form factors in the Δ production region, there are disagreements between theory and experimental data, and the Δ production region still needs further studies [15].

*liujian@upc.edu.cn

Another key problem in (e, e') scattering is accurate calculations of spectral function. The theoretical calculations of the spectral function $S(\mathbf{p}, E)$ can be assumed to consist of the MF part $S_{\text{MF}}(\mathbf{p}, E)$ and the NN -SRC part $S_{\text{corr}}(\mathbf{p}, E)$ [10,14,16]. The MF part $S_{\text{MF}}(\mathbf{p}, E)$ gives the descriptions that the nucleons move in well-defined quantum states, under the effect of an average field created by their interactions. Compared with the $S_{\text{MF}}(\mathbf{p}, E)$, the NN -SRC part $S_{\text{corr}}(\mathbf{p}, E)$ provides supplementary description of nucleons with high momentum and high removal energy above the Fermi surface, which are caused by tensor attraction and short-range repulsion. The *ab initio* method [17,18] is a fundamental method to describe the NN -SRC of light nuclei, but it is still difficult to apply to the medium and heavy nuclei. Because the NN -SRC is unaffected by surface and shell effects [3], the $S_{\text{corr}}(\mathbf{p}, E)$ of the finite nuclei can be evaluated from rescaling the strength of NN -SRC of deuteron [19].

In this paper, the (e, e') scattering theory is linked with the microscopic nuclear structure model, and the influences of NN -SRC on the (e, e') cross sections are studied. In the calculations of Δ production scattering, the appropriate form factors are used, in addition, the conservation of energy and momentum in the scattering process and the decay width of $\Delta(1232)$ are also considered. Therefore, the calculation results have been significantly improved. On the basis of theoretical results, we study the effect of the NN -SRC part and the mean-field part on the (e, e') cross sections, respectively. Furthermore, this paper analyzes the sensitivity of the inclusive electron scattering to the NN -SRC at the different kinematics. Finally, another method is proposed to extract the strength of NN -SRC from the experimental cross sections.

Formulas. The calculations of spectral function in this paper are divided into two categories: the MF part $S_{\text{MF}}(\mathbf{p}, E)$ and the $S_{\text{corr}}(\mathbf{p}, E)$

$$S(\mathbf{p}, E) = S_{\text{MF}}(\mathbf{p}, E) + S_{\text{corr}}(\mathbf{p}, E), \quad (1)$$

with the normalization requirement $\int d^3p dE S(\mathbf{p}, E) = A$. In this paper, the MF parts are calculated by the axially deformed relativistic mean-field (RMF) model. At low energy E and low momentum \mathbf{p} , the MF part $S_{\text{MF}}(\mathbf{p}, E)$ is dominated by the single-particle properties,

$$S_{\text{MF}}(\mathbf{p}, E) = \sum_i C_i (|f_i(\mathbf{p})|^2 + |g_i(\mathbf{p})|^2) L_i(E - E_i), \quad (2)$$

where $f_i(\mathbf{p})$ and $g_i(\mathbf{p})$ are the two-dimensional Dirac spinors in momentum space for the single-particle state i , and C_i is the corresponding occupation number of the single-particle state i . The finite width in energy dependence can be described by Lorentzian function L_i [20].

At the region of high energy E and high momentum \mathbf{p} , the NN -SRC part $S_{\text{corr}}(\mathbf{p}, E)$ plays a leading role because the strong dynamical NN -SRC leads to virtual scattering processes exciting the nucleons to the states above the Fermi surface. The $S_{\text{corr}}(\mathbf{p}, E)$ is determined by ground-state configurations with the NN -SRC pair and the $(A - 2)$ nucleon residual system. The NN -SRC pair has a high relative momentum \mathbf{p}_{rel} and a low center-of-mass momentum $\mathbf{p}_{\text{c.m.}}$. At the region of high \mathbf{p} , the NN -SRC momentum distribution originates from the relative momentum distribution

$n_{\text{corr}}(\mathbf{p}) = n_{\text{rel}}(\mathbf{p})$, because of the low center-of-mass momentum. Assuming the $n_{\text{c.m.}}(\mathbf{p}_{\text{c.m.}}) = (\alpha/\pi)^{3/2} \exp(-\alpha \mathbf{p}_{\text{c.m.}}^2)$, the $S_{\text{corr}}(\mathbf{p}, E)$ can be obtained by the integral of $\mathbf{p}_{\text{c.m.}}$ [16]

$$S_{\text{corr}}(\mathbf{p}, E) = n_{\text{corr}}(\mathbf{p}) \frac{m}{|\mathbf{p}|} \sqrt{\frac{\alpha}{\pi}} \times [\exp(-\alpha \mathbf{p}_{\text{min}}^2) - \exp(-\alpha \mathbf{p}_{\text{max}}^2)], \quad (3)$$

where the $\alpha = 3/[4(\mathbf{p}^2)(A - 2)/(A - 1)]$. The \mathbf{p}_{min} and the \mathbf{p}_{max} are the lower and upper limits of the $\mathbf{p}_{\text{c.m.}}$.

There are many microscopic or phenomenological methods to calculate the $n_{\text{corr}}(\mathbf{p})$, and the light-front dynamics (LFD) method is adopted in this paper. In the LFD method, the $n_{\text{corr}}(\mathbf{p})$ can be obtained by rescaling the NN -SRC part of the precise momentum distribution of deuteron. The momentum distribution can be expressed as follows:

$$n_{\text{corr}}^{\tau}(\mathbf{p}) = N_{\tau} \tau C_A [n_2(\mathbf{p}) + n_5(\mathbf{p})], \quad (4)$$

where the two components $n_2(\mathbf{p})$ and $n_5(\mathbf{p})$ reflect of deuteron, which are deduced from LFD wave functions [21]. The $n_2(\mathbf{p})$ term is mainly induced by the tensor force, the $n_5(\mathbf{p})$ term is mainly induced by the π exchange [22]. The scaling factor C_A is the ratio of high-momentum components between other nuclei and deuteron. For different nuclei, the scaling factor C_A represents the strength of NN -SRC, which needs to be extracted by electron scattering.

During the inclusive electron scattering (e, e') process, the incident electrons are interacted with the target nucleus and scattered off from four-momentum $k \equiv (E_{\mathbf{k}}, \mathbf{k})$ to $k' \equiv (E_{\mathbf{k}'}, \mathbf{k}')$. The four-momentum transfer of scattered electrons is $q \equiv (\omega, \mathbf{q})$. Neglecting the final-state interactions, the double differential cross sections can be written as [14]

$$\frac{d^2\sigma}{d\Omega dE_{\mathbf{k}'}} = \frac{\alpha^2 E_{\mathbf{k}'}}{Q^4 E_{\mathbf{k}}} L_{\mu\nu} W^{\mu\nu}, \quad (5)$$

where α is the fine structure constant and the squared four-momentum transfer $Q^2 = -q^2 = \omega^2 - \mathbf{q}^2$. In Eq. (5), the leptonic tensor $L_{\mu\nu}$ is completely determined by the electron kinematics, and the nuclear tensor $W^{\mu\nu}$ includes all the information of target nuclear

$$W^{\mu\nu} = \sum_X \langle 0 | J^{\mu} | X \rangle \langle X | J^{\nu} | 0 \rangle \delta^{(4)}(p_0 + q - p_X), \quad (6)$$

where J^{μ} is nuclear currents, and p_0 and p_X are the four-momentums of hadronic initial states and final states. In the impulse approximation (IA) scheme, the scattering process is considered the incoherent sum of elementary scattering reaction involving only one nucleon. Therefore, the nuclear tensor can be described as

$$W^{\mu\nu} = \sum_i \int d^3p dE w_i^{\mu\nu}(\tilde{q}) \left(\frac{m}{E_{\mathbf{p}}} \right) S(\mathbf{p}, E). \quad (7)$$

The nucleon tensor $w_i^{\mu\nu}$ reflects the electromagnetic interactions of a bound nucleon carrying momentum \mathbf{p} .

Combining with Eqs. (5) and (7), the (e, e') cross sections can be written in the form

$$\frac{d^2\sigma}{d\Omega dE_{\mathbf{k}'}} = \int d^3p dE \left[S_p(\mathbf{p}, E) \frac{d^2\sigma_{ep}}{d\Omega dE_{\mathbf{k}'}} + S_n(\mathbf{p}, E) \frac{d^2\sigma_{en}}{d\Omega dE_{\mathbf{k}'}} \right] \delta(\omega - E + m - E_{|\mathbf{p}+\mathbf{q}|}), \quad (8)$$

where the elementary cross section $d^2\sigma_{eN}/d\Omega dE_{\mathbf{k}'}$ represents the scattering of an electron by a nucleon for the QE and the Δ production process [14]. We calculate the $d^2\sigma_{eN}/d\Omega dE_{\mathbf{k}'}$ using the form factors in QE process [14] and the Δ production process [23], which reflect the electromagnetic structure of the nucleon and the $\Delta(1232)$. For the integration process, we determine the limits of integration by considering the conservation of energy and momentum in the scattering process.

In particular, for the Δ production process, the Lorentzian shape Δ width is used as a substitute for the energy-conserving δ function in Eq. (8) to produce a broadening of the Δ peak and correspondingly a decrease of the strength

$$\delta \rightarrow \frac{1}{\pi} \frac{\Gamma(W)/2}{(W - m_\Delta)^2 + \Gamma(W)^2/4}, \quad (9)$$

where the parameter W is the invariant mass. The parameter $\Gamma(W)$ is the decay width of $\Delta(1232)$ [23]. The integration interval of W goes from threshold to the maximum value allowed in the Fermi gas model $m + m_\pi < W < \sqrt{(E_F + \omega)^2 - (q - p_F)^2}$.

Momentum distribution and spectral function. The nucleon momentum distributions $n(p)$ and the nuclear spectral functions $S(p, E)$ are calculated with the formulas above. The corresponding nuclear wave functions in momentum space are obtained from the axially deformed RMF model with the NL3* parameter set. The correlation part $S_{\text{corr}}(p, E)$ is obtained from the LFD method with the strength $C_A = 4.5$ in Eq. (4).

In Fig. 1(a), we present the logarithm of spectral function $S(p, E)$ of ^{56}Fe to highlight the NN -SRC part. We observed that in the region of high removal energy ($E > 100$ MeV) and high momentum ($p > 1.5$ fm $^{-1}$), the spectral function is mainly from the contributions of NN -SRC, which has no shell structure and shows in a smooth ridge. Unlike the NN -SRC part, one can clearly distinguish the different orbits from the mean-field $S_{\text{MF}}(p, E)$ in the region of $E < 90$ MeV and $p < 1.5$ fm $^{-1}$ (region enclosed by a curve). The corresponding nucleon momentum distribution $n(p)$ of ^{56}Fe are calculated by $S(p, E)$ and presented in Fig. 1(b). The momentum distribution extracted from the (e, e') cross sections and analyzed in terms of y scaling in Refs. [24,25] are also provided in this figure for comparison. From Fig. 1(b), the mean-field calculations only provide good descriptions on $n(p)$ below the Fermi momentum $p_F \approx 1.39$ fm $^{-1}$. For $p > p_F$, the $n(p)$ from the pure mean-field calculations decrease rapidly and deviate from the $n(p)$ from the y -scaling analyses. By considering the NN -SRC contributions, the value of $n(p)$ on the tail is enhanced and consistent with the result of the y -scaling analyses.

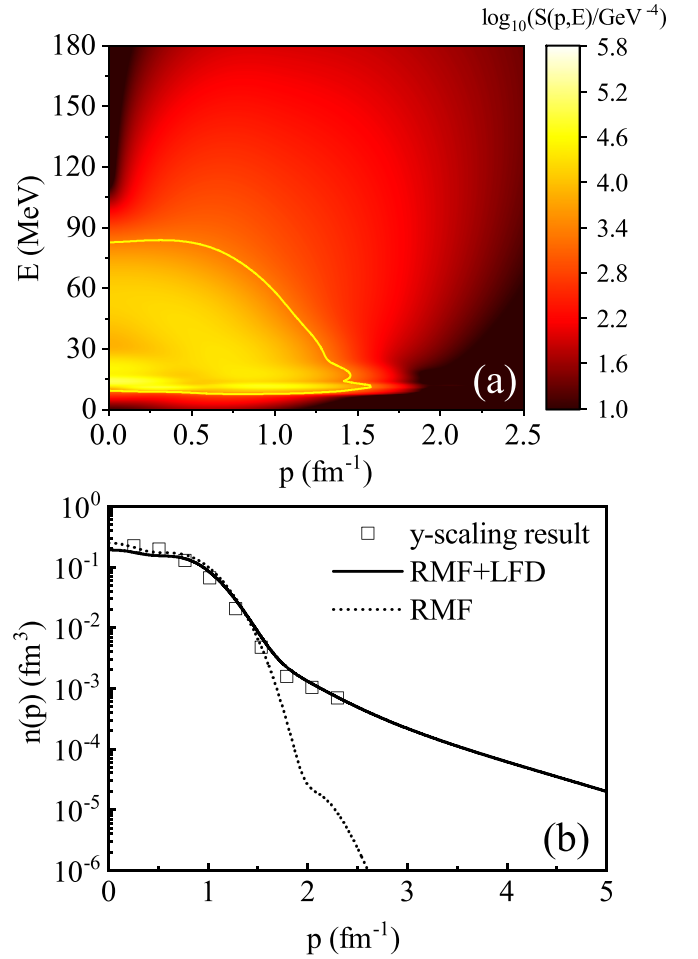


FIG. 1. Momentum distribution $n(p)$ and spectral functions $S(p, E)$ of ^{56}Fe for the deformation $\beta = 0.17$ calculated from the deformed RMF model with the LFD method. In Fig. 1(a), the logarithm of $S(p, E)$ is presented to highlight the NN -SRC part, and the region enclosed by a curve describes the mean-field part. The open squares represent the $n(p)$ obtained from y -scaling analyses on (e, e') cross sections [25].

Inclusive electron scattering cross sections. In Fig. 2, we present theoretical (e, e') cross sections of ^{56}Fe from the spectral function of Fig. 1(a). The theoretical results of the inclusive electron scattering can be divided into the QE peak and Δ production peak. Good agreements with the experimental data are obtained in the total theoretical cross sections. Especially for the Δ production region, we observed that the location and the value of the experimental peak can be reproduced well by Eqs. (8) and (9). The calculations of Δ production cross sections rely on the nucleon structure functions including the magnetic, electric, and Coulomb excitation form factors. Thus, the Δ production peak contains information about the nucleon's excited states and the electromagnetic structure of $\Delta(1232)$ baryon, which is beneficial for understanding strong interactions in the domain of quark confinement.

Both the QE scattering and Δ production scattering follow the energy and momentum conservations. The QE peak

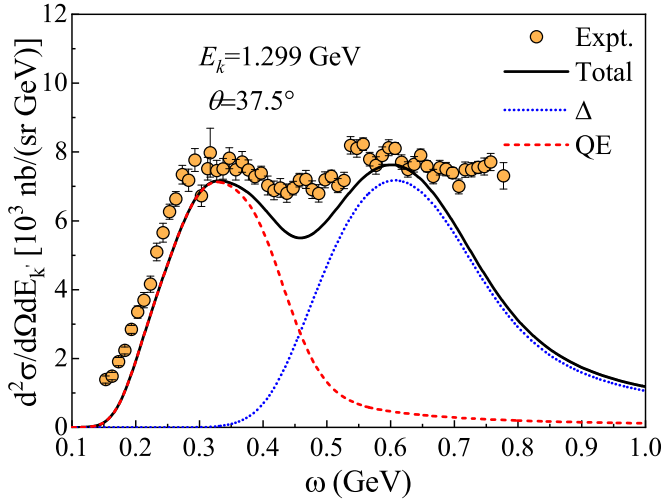


FIG. 2. The total (e, e') cross sections of ^{56}Fe calculated by PWIA method at the kinematics $E_k = 1.299$ GeV and $\theta = 37.5^\circ$, where the spectral function is from RMF+LFD calculations. The experimental data are from Ref. [26]. Dotted lines, the cross sections of the Δ production peaks; dashed lines, the cross sections of the QE peaks.

locates at the energy transfer $\omega_{QE} = Q^2/2m = 0.33$ GeV, which reflects the process of the electron scattered by a free nucleon [27]. For the Δ production scattering, the peak locates at $\omega_\Delta = m_\Delta - m + \omega_{QE} = 0.62$ GeV, which corresponds to the excitation of a free nucleon to form a $\Delta(1232)$.

Effects of NN-SRC. In this part, we further separate the (e, e') cross sections into the MF part and the NN -SRC part. The results of ^{56}Fe are exhibited in Fig. 3, calculated with the kinematics $E_k = 1.108$ GeV and $\theta = 37.5^\circ$. For the strength of NN -SRC, the corresponding proportion of high-momentum

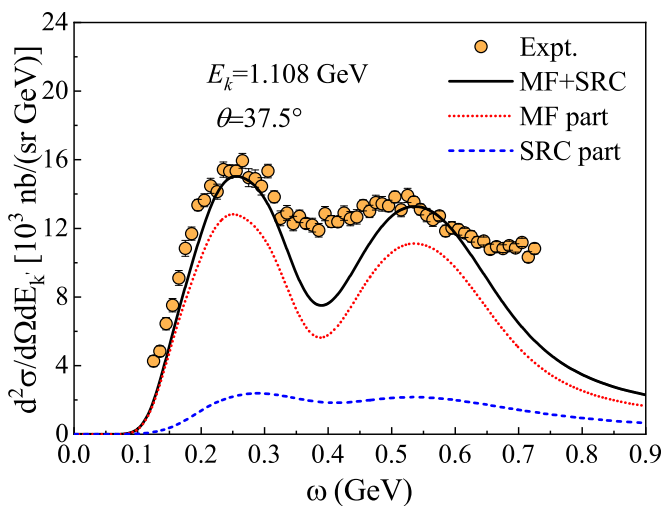


FIG. 3. The (e, e') cross sections of ^{56}Fe at the kinematics $E_k = 1.108$ GeV and $\theta = 37.5^\circ$, calculated with the $S(p, E)$ of Fig. 1(a). Solid line, the total inclusive cross sections. Dotted line, the contributions of MF part. Dashed line, the contributions of NN -SRC part. The experimental data are from the Ref. [28].

nucleons is $Y = 21.4\%$ in total nucleon number. However, in Fig. 3 the contributions of NN -SRC part to the total cross sections are about 16%. It means that parts of the NN -SRC nucleons with high E and p cannot take part in the (e, e') reaction, because of the conservation of momentum and energy. With the increase of incident energy and angle, the contributions of NN -SRC nucleons to the total cross sections are enhanced. Therefore, it is suitable to extract the strength of NN -SRC from the (e, e') reaction at the kinematics with high Q^2 .

It was pointed out that the ratio of the (e, e') cross sections per nucleon of nucleus A to that of deuterium have a plateau [11–13], in the range of the Bjorken scaling variable $1.5 < x_B < 2$ and the squared four-momentum transfer $Q^2 > 2$ GeV 2 . At this condition, the (e, e') cross sections are mainly from the NN -SRC nucleons, and the contributions of mean-field nucleons can be negligible because of the energy and momentum conservations. From the analyses of Fig. 3, we also found that the kinematics with high Q^2 are suitable to extract the strength of NN -SRC, which agrees with previous studies.

Extract the strength of the NN-SRC. In Fig. 4, we present the inclusive cross sections of ^{16}O , ^{27}Al , ^{56}Fe , and ^{186}W calculated by the spectral function for the different strength of NN -SRC. To extract the information of NN -SRC form nuclei, we choose the squared four-momentum transfer ranges from 0.5 to 1 GeV 2 , and the corresponding kinematics are given in Fig. 4. From Fig. 4, one can observe there are noticeable changes of (e, e') cross sections near the QE and Δ production peaks for different correlation strength. For ^{16}O in Fig. 4(a), the correlation strengths are $C_A = 1.0, 4.2,$ and 8.0 , and the high-momentum nucleons account for 6.5%, 22.4%, and 35.2% in total nucleon number, respectively. Comparing the theoretical (e, e') cross sections with the experimental data, the strengths of NN -SRC are constrained to be $C_A = 4.2$ for ^{16}O , which indicates the correlated nucleons contribute to about 22.4% of the total nucleon number. For ^{27}Al , ^{56}Fe , and ^{186}W , the corresponding analysis are also carried out. Finally, we obtain that the strengths of NN -SRC are $C_A = 5.3$ for ^{27}Al , $C_A = 4.5$ for ^{56}Fe , and $C_A = 5.0$ for ^{186}W . The percentages of high-momentum nucleons in total nucleon number are $Y = 25.5\%$ for ^{27}Al , $Y = 21.4\%$ for ^{56}Fe , and $Y = 20.2\%$ for ^{186}W . In this analysis, we found that the correlated terms contribute to about 20% of the total nucleon in medium and heavy nuclei, which verifies the *ab initio* calculation from Ref. [31] and is consistent with the result from exclusive electron scattering in Refs. [7,8].

In previous (e, e') studies [11–13], at the region $1.5 < x_B < 2$ the strengths of NN -SRC are also extracted to be 5.2 for ^{56}Fe and 5.3 for ^{27}Al from the plateau of the ratios of (e, e') cross sections between heavy nuclei and the deuteron. The method of extracting the strengths of NN -SRC from the plateau can remove interference of the mean-field part. However, this region $1.5 < x_B < 2$ corresponds to a narrow range of low energy transfer, as shown in the shaded area of Figs. 4(b) and 4(c). At kinematics $Q^2 > 2$ GeV 2 , the QE peak and Δ production peak are not obvious, and the deep inelastic scattering (DIS) plays a dominate role in total (e, e') cross sections, which is sensitive to the internal structure of

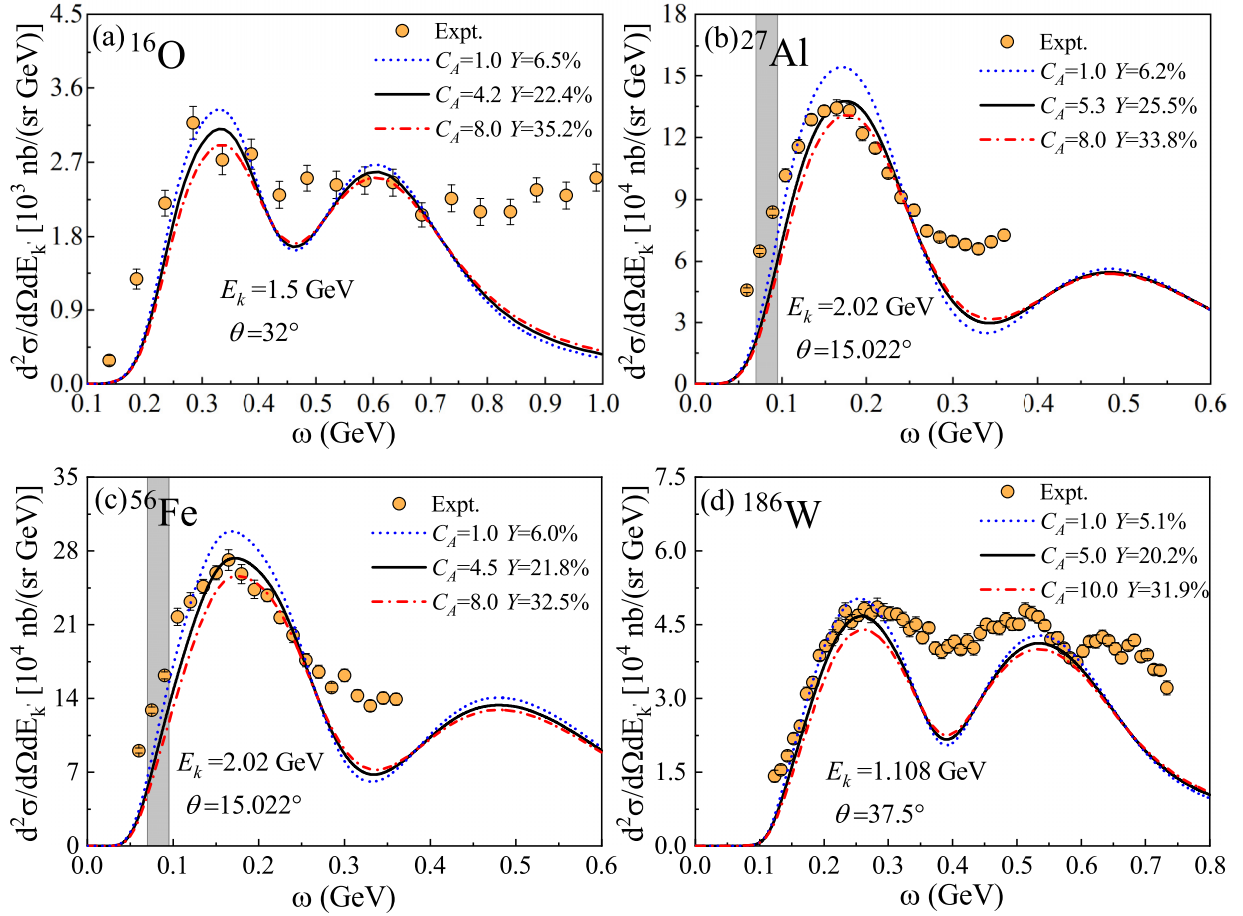


FIG. 4. (a) The inclusive cross sections of ^{16}O at the kinematic $E_k = 1.5$ GeV and $\theta = 32^\circ$ for different NN -SRC strengths, calculated from the spectral function from RMF+LFD method. (b) Same as panel (a) but for ^{27}Al at the kinematic $E_k = 2.02$ GeV and $\theta = 15.022^\circ$. (c) Same as panel (a) but for ^{56}Fe at the kinematic $E_k = 2.02$ GeV and $\theta = 15.022^\circ$. (d) Same as panel (a) but for ^{186}W at the kinematic $E_k = 1.108$ GeV and $\theta = 37.5^\circ$. The shaded areas in panels (b) and (c) represent the region of the Bjorken scaling variable $1.5 < x_B < 2$. The experimental data are from Refs. [26,29,30].

a proton or neutron. In Fig. 4 of this paper, the Q^2 region $0.5\text{--}1$ GeV 2 is selected for different nuclei. One can see that at this kinematics, the inclusive cross sections are mainly from the contributions of QE process and Δ production process, which can better reflect the information of NN -SRC effects and mean-field structure in nuclei.

Summary. The short-range correlation is an important nuclear property associated with the high-momentum components of the nuclear momentum distributions. In this paper, the effects of NN -SRC on the inclusive electron scattering process are systematically studied, where the nuclear spectral functions are obtained from the combinations of the deformed RMF model and the LFD method. By using the appropriate form factors and the decay width, we improve the theoretical cross sections in the Δ production region.

We further separate (e, e') cross sections into MF and the NN -SRC parts. One can see that the increase of NN -SRC strength causes a reduction of the cross sections near the QE and the Δ production peaks. By the method proposed in this paper, the strength of NN -SRC for the ^{16}O , ^{27}Al , ^{56}Fe , and

^{186}W are constrained from the experimental data at suitable kinematics to be $C_A = 4.2, 5.3, 4.5,$ and 5.0 , respectively, which correspond the proportions of high-momentum nucleons $Y = 22.4\%, 25.5\%, 21.4\%,$ and 20.2% .

The research in this paper can help to distinguish the nuclear effects and beyond the standard model effects in neutrino-nucleus scattering experiments. Furthermore, the studies are useful for understanding the nuclear structure and comprehending the strong interactions.

Acknowledgments. This work was supported by the National Natural Science Foundation of China (Grants No. 11505292, No. 11822503, No. 11975167, No. 11961141003, and No. 12035011), by the Shandong Provincial Natural Science Foundation, China (Grant No. ZR2020MA096), by the Open Project of Guangxi Key Laboratory of Nuclear Physics and Nuclear Technology (Grant No. NLK2021-03), and by the Key Laboratory of High Precision Nuclear Spectroscopy, Institute of Modern Physics, Chinese Academy of Sciences (Grant No. IMPKFKT2021001).

- [1] O. Hen, B.-A. Li, W.-J. Guo, L. B. Weinstein, and E. Piasetzky, *Phys. Rev. C* **91**, 025803 (2015).
- [2] B.-A. Li, B.-J. Cai, L.-W. Chen, and J. Xu, *Prog. Part. Nucl. Phys.* **99**, 29 (2018).
- [3] O. Hen, G. A. Miller, E. Piasetzky, and L. B. Weinstein, *Rev. Mod. Phys.* **89**, 045002 (2017).
- [4] M. Duer, A. Schmidt, J. R. Pybus, E. P. Segarra, A. Hrnjic, A. W. Denniston, R. Weiss, O. Hen, E. Piasetzky, L. B. Weinstein *et al.*, *Phys. Rev. Lett.* **122**, 172502 (2019).
- [5] M. Duer, O. Hen, E. Piasetzky, H. Hakobyan, L. B. Weinstein, M. Braverman, E. O. Cohen, D. Higinbotham, K. P. Adhikari, S. Adhikari *et al.* (CLAS Collaboration), *Nature (London)* **560**, 617 (2018).
- [6] B. Schmookler, M. Duer, A. Schmidt, O. Hen, S. Gilad, E. Piasetzky, M. Strikman, L. B. Weinstein, S. Adhikari, M. Amaryan *et al.* (CLAS Collaboration), *Nature (London)* **566**, 354 (2019).
- [7] R. Subedi, R. Shneur, P. Monaghan, B. D. Anderson, K. Aniol, J. Annand, J. Arrington, H. Benaoum, F. Benmokhtar, W. Boeglin *et al.*, *Science* **320**, 1476 (2008).
- [8] O. Hen, M. Sargsian, L. B. Weinstein, E. Piasetzky, H. Hakobyan, D. W. Higinbotham, M. Braverman, W. K. Brooks, S. Gilad, K. P. Adhikari *et al.*, *Science* **346**, 614 (2014).
- [9] R. Schiavilla, R. B. Wiringa, S. C. Pieper, and J. Carlson, *Phys. Rev. Lett.* **98**, 132501 (2007).
- [10] C. Ciofi degli Atti, *Phys. Rep.* **590**, 1 (2015).
- [11] L. L. Frankfurt, M. I. Strikman, D. B. Day, and M. Sargsyan, *Phys. Rev. C* **48**, 2451 (1993).
- [12] K. S. Egiyan, N. B. Dashyan, M. M. Sargsian, M. I. Strikman, L. B. Weinstein, G. Adams, P. Ambrozewicz, M. Anghinolfi, B. Asavapibhop, G. Asryan *et al.*, *Phys. Rev. Lett.* **96**, 082501 (2006).
- [13] N. Fomin, J. Arrington, R. Asaturyan, F. Benmokhtar, W. Boeglin, P. Bosted, A. Bruell, M. H. S. Bukhari, M. E. Christy, E. Chudakov *et al.*, *Phys. Rev. Lett.* **108**, 092502 (2012).
- [14] O. Benhar, D. Day, and I. Sick, *Rev. Mod. Phys.* **80**, 189 (2008).
- [15] O. Benhar and D. Meloni, *Phys. Rev. Lett.* **97**, 192301 (2006).
- [16] S. A. Kulagin and R. Petti, *Nucl. Phys. A* **765**, 126 (2006).
- [17] S. C. Pieper and R. B. Wiringa, *Annu. Rev. Nucl. Part. Sci.* **51**, 53 (2001).
- [18] N. Wan, T. Myo, C. Xu, H. Toki, H. Horiuchi, and M. Lyu, *Chin. Phys. C* **44**, 124104 (2020).
- [19] A. N. Antonov, M. K. Gaidarov, M. V. Ivanov, D. N. Kadrev, G. Z. Krumova, P. E. Hodgson, and H. V. von Geramb, *Phys. Rev. C* **65**, 024306 (2002).
- [20] M. V. Ivanov, A. N. Antonov, G. D. Megias, J. A. Caballero, M. B. Barbaro, J. E. Amaro, I. RuizSimo, T. W. Donnelly, and J. M. Udias, *Phys. Rev. C* **99**, 014610 (2019).
- [21] J. Carbonell and V. A. Karmanov, *Nucl. Phys. A* **581**, 625 (1995).
- [22] X. Wang, Q. Niu, J. Zhang, M. Lyu, J. Liu, C. Xu, and Z. Ren, *Sci. China: Phys., Mech. Astron.* **64**, 292011 (2021).
- [23] J. E. Amaro, M. B. Barbaro, J. A. Caballero, T. W. Donnelly, and A. Molinari, *Nucl. Phys. A* **657**, 161 (1999).
- [24] C. Ciofi degli Atti, E. Pace, and G. Salmè, *Phys. Rev. C* **36**, 1208 (1987).
- [25] C. Ciofi degli Atti, E. Pace, and G. Salmè, *Phys. Rev. C* **43**, 1155 (1991).
- [26] R. M. Sealock, K. L. Giovanetti, S. T. Thornton, Z. E. Meziani, O. A. Rondon-Aramayo, S. Auffret, J. P. Chen, D. G. Christian, D. B. Day, J. S. McCarthy, R. C. Minehart, L. C. Dennis, K. W. Kemper, B. A. Mecking, and J. Morgenstern, *Phys. Rev. Lett.* **62**, 1350 (1989).
- [27] L. Wang, J. Liu, R. Wang, M. Lyu, C. Xu, and Z. Ren, *Phys. Rev. C* **103**, 054307 (2021).
- [28] J. P. Chen, Z. E. Meziani, D. Beck, G. Boyd, L. M. Chinitz, D. B. Day, L. C. Dennis, G. Dodge, B. W. Filippone, K. L. Giovanetti, J. Jourdan, K. W. Kemper, T. Koh, W. Lorenzon, J. S. McCarthy, R. D. McKeown, R. G. Milner, R. C. Minehart, J. Morgenstern, J. Mougey *et al.* *Phys. Rev. Lett.* **66**, 1283 (1991).
- [29] M. Anghinolfi, M. Battaglieri, N. Bianchi, R. Cenni, R. Corvisiero, A. Fantoni, R. Levi Sandri, A. Longhi, V. Lucherini, V. I. Mokeev *et al.*, *Nucl. Phys. A* **602**, 405 (1996).
- [30] D. B. Day, J. S. McCarthy, Z. E. Meziani, R. Minehart, R. Sealock, S. T. Thornton, J. Jourdan, I. Sick, B. W. Filippone, R. D. McKeown, R. G. Milner, D. H. Potterveld, Z. Szalata *et al.*, *Phys. Rev. C* **48**, 1849 (1993).
- [31] M. Lyu, T. Myo, H. Toki, H. Horiuchi, C. Xu, and N. Wan, *Phys. Lett. B* **805**, 135421 (2020).